터널과 지하공간, 한국암반공학회
Vol. 11, No. 4, 2001, pp. 301~310

TUNNEL & UNDERGROUND Vol. 11, No. 4, 2001, pp. 301-310
J. of Korean Society for Rock Mech.

일축압축 상태하 다중 불연속면의 파괴에 대한 연구

사공 명[1] · 안토니오 보베[2]

Fracture of Multiple Flaws in Uniaxial Compression

Myung Sagong and Bobet Antonio

Abstract. Gypsum blocks with sixteen flaws have been prepared and tested in uniaxial compression. Results from these experiments are compared with observations from the same material with two and three flaws. The results indicate that the cracking pattern observed in specimens with multiple flaws is analogous to the pattern obtained in specimens with two and three flaws such as initiation and propagation of wing, and secondary cracks and coalescence. Wing cracks initiate at an angle with the flaw and propagate in a stable manner towards the direction of maximum compression. Secondary cracks initiate and propagate in a stable manner. As the load is increased, secondary cracks may propagate in an unstable manner and produce coalescence. Two types of secondary cracks are observed: quasi-coplanar, and oblique secondary cracks. Coalescence is produced by the linkage of two flaws: wing and/or secondary cracks. From the sixteen flaws test, four types of coalescence are observed. Observed types of coalescence and initiation stress of wing and secondary cracks depend on flaw geometries, such as spacing, continuity, flaw inclination angle, ligament angle, and steppings.

Keywords: Uniaxial compression, Coalescence, Wing crack, Quasi-coplanar secondary crack, Oblique secondary crack, Right and left stepping, Overlapping and non-overlapping, Ligament.

초 록. 열여섯개의 절리면을 가진 석고 시편을 제작, 일축 압축 실험을 하여 관측된 결과를 절리면이 두 개 및 세 개 가진 시편의 실험 결과와 비교하였다. 그 결과 다중 절리면(열여섯 면)에서 관측된 익형(翼形) 크랙, 이차 크랙, 연절리(連節理) 유형은 절리가 두 개 및 세 개를 가진 시험체와 비슷한 형상을 보였다. 익형 크랙은 절리면과 일정한 각도를 유지한 상태에서 시작하여 안정적으로 진전, 최대 압축응력 방향으로 발달하였으며 이차 크랙 또한 안정적인 진전 양상을 보였으나 높은 하중 상태에서 이차 크랙은 불안정한 진전을 보이며 연절리 현상을 보였다. 이차 크랙의 종류로는 유사 공면(共面) 및 사면(斜面) 이차 크랙이 관측되었다. 연절리 현상은 익형 크랙과 이차 크랙에 의한 절리면의 연결로 나타나며 본 실험에서 네 종류의 연절리 현상이 관측되었다. 관측된 연절리의 발생 형태, 익형 크랙 및 이차 크랙의 초기 발생 응력은 절리면의 간격, 연속성, 경사각, 단선(短線) 각도와 절리면의 배열과 관련이 있다.

핵심어: 일축압축하중, 연절리(連節理), 익형(翼形) 크랙, 유사공면(共面) 이차 크랙, 사면(斜面) 이차 크랙, 우향 및 좌향 충상 배열, 중복 및 비중복형 배열, 단선(短線).

1. Introduction

Rock, as an engineering material, has particular properties with its discontinuities such as joints, faults, beddings, and foliation. Generally, rock contains discontinuities at any scale due to its origination processes: mechanical, and thermal processes. Mostly, the processes form multiple numbers of discontinuities along the similar orientation. With the existence of discontinuities, the internal stress distribution of rock mass severely depends upon geometrical distribution of discontinuities. The perturbation induced by existing discontinuities in the rock masses depends on the size, orientation, opening (aperture), numbers, persistence, and roughness of discontinuities. Existence of discontinuities in rock masses may change ultimate strength, elastic modulus, deformability, thermal conductivity, and hydraulic conductivity of rock masses. Considerable amount of works have been performed on the initiation of the crack from the tip of single flaw in brittle materials based on fracture mechanics. These works provide valuable under-

[1]퍼듀대학교 토목공학과 박사 과정
[2]퍼듀대학교 토목공학과 교수
접수일 : 2001년 8월 29일
심사 완료일 : 2001년 11월 13일

standing on the fracture of rocks, which have quasi-brittle characteristics. However, the types of cracks observed in rocks are in multiple along similar orientation and characteristics. Observation on the single flaw may provide limited view of entire fracturing. Hence, the drive on the experiments on multiple discontinuities is accelerated. As shown in past works,[1-3] failure of rock-structure is partially induced by coalescence, linkage of discontinuities. Under the compression, fractured rock can maintain strength of the material during excessive non-elastic response. Progress of rock fracturing would be completed right before the entire failure of specimens. Up to this point of loading, coalescence can occur and accumulate damage in the rock masses. Therefore, it is crucial to understand the processes of coalescence.

Systematic observations on the coalescence of two and three discontinuities have been performed on rock models.[4-7] In fact, the discontinuities in nature are grouped as sets or arrays of them thus, the study on the multiple number of flaws is necessary to be more realistic. Furthermore, the intention of multiple flaw tests is to show any similarity or difference, between past works[4-7] on two and three flaws, and multiple (sixteen) flaws in rock-model. With coale-scence, initiation and propagation processes will be investigated concurrently. Uniaxial compression is applied for the test. This paper will revisit the results of three flaws test and make a comparison of the results of sixteen flaws and two and thee flaw tests.

2. Geometries of Flaws

Specimens used for the tests are made of the mixture of gypsum, water and diatomaceous earth. The proportions used are following: water/gypsum = 0.4, and water/diatomaceous earth = 35.0. The physical properties of this rock-model have been extensively studied[8] and the model has been successfully applied on the experiments for the effects of discontinuities on rock masses.[4-7]

The size of specimens is 203.2 mm × 101.6 mm × 30.0 mm (Figure 1(a)). The dimensions of the flaws are 12.7 mm wide, and 0.1 mm thick. The specimens contain sixteen flaws by forming four columns and rows (see Figure 1(a)). The length of flaws is the same,

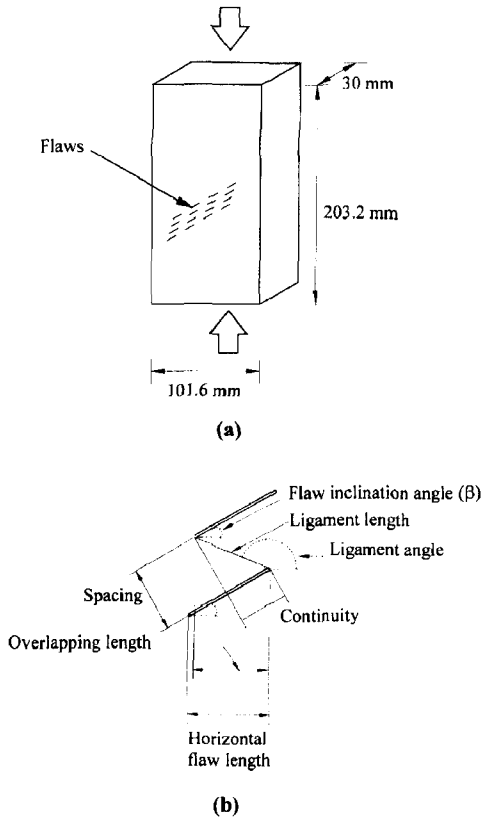

Fig. 1. Specimen with multiple flaws; (a) Overall view, (b) detail view.

12.7 mm, and the flaws are parallel. The distance between contiguous columns of flaws is the same with the length of flaw: 12.7 mm. The flaw geometry is defined by three parameters, spacing (S), continuity (C), and flaw inclination angle (β); see Figure 1(b).

Spacing and continuity are represented by "a", a half-length of flaw (6.35 mm). Spacing is the perpendicular distance between adjacent flaws in the same column. Two different spacings are used; "a", and "2a" (i.e. 6.35 mm and 12.7 mm, respectively). Continuity is the planar distance between adjacent flaws, and is defined as the overlapping length between two flaws measured along the plane of the flaws (see Figure 1(b)). Continuity can be either positive, or negative. When upper and lower flaws overlap as in Figure 1(b), continuity for this case is positive. Likewise, when they are non-overlap geometry, continuity is negative. Four continuities are employed:

"-a", "0", "a", and "2a" (i.e. -6.35 mm, 0 mm, 6.35 mm and 12.7 mm). Flaw inclination angle is the angle measured from flaw plane to the horizontal direction. Three different flaw inclination angles are used, 30°, 45°, and 60°. The three parameters are combined to describe particular geometry of specimens: SCβ; for example, a2a30° corresponds to a flaw geometry with spacing "a", continuity "2a", and flaw inclination angle 30°.

Overlapping ratio is used to show the geometry effects on crack initiation.[7] Overlapping ratio is the percentage of overlapped part of two flaws with respect to projected flaw length in horizontal direction (i.e. 2a cos β) (see Figure 1(b)). This ratio varies with the change of flaw inclination angle. Overlapping ratio of non-overlapping geometries is negative.

Depending on their relative locations, two flaws may overlap in the direction of loading (overlapping geometries), or may not overlap (non-overlapping geometries); see Figure 2. In addition, overlapping and non-overlapping may occur either with left stepping or with right stepping. A right or left stepping geometry occurs when, along the direction of loading, one moves from the top flaw to the bottom flaw stepping down to the right or to the left, respectively. The arrows drawn in Figure 2 show stepping of each flaw array: when an arrow directs towards left or right direction, the flaw arrays are left or right stepping, respectively. Ligament is the shortest line connecting the tips of two flaws thus ligament length is the distance between the tips of two flaws. Ligament angle is the angle measured from horizontal direction to the ligament. Ligament

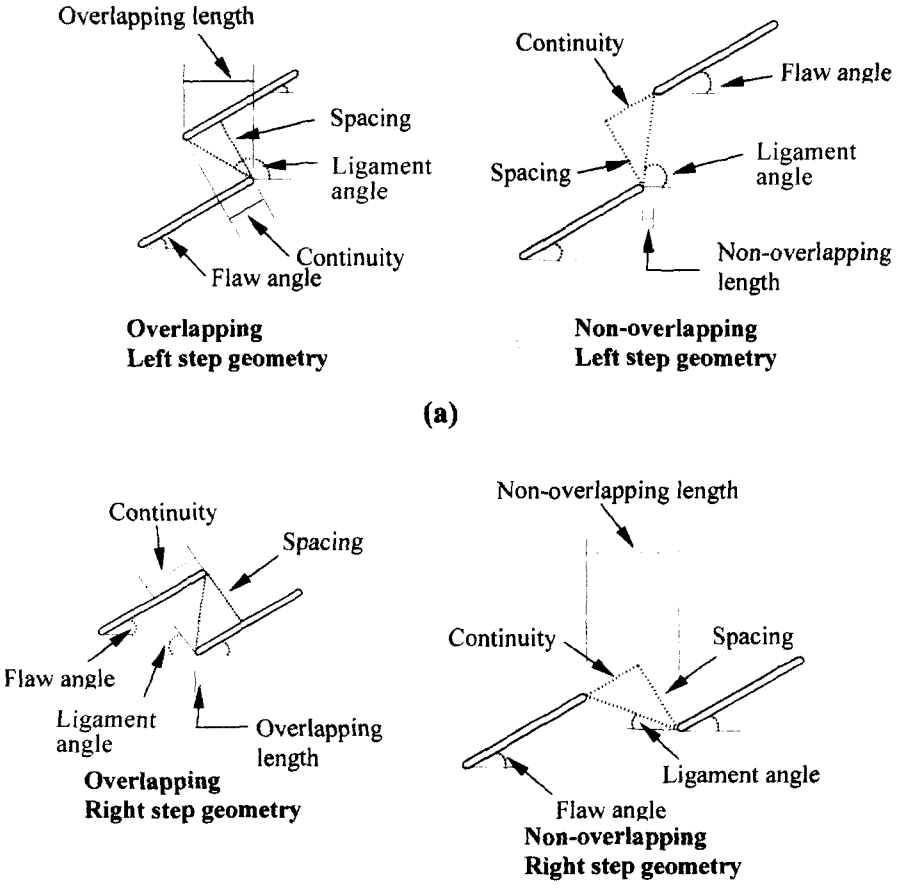

Fig. 2. Flaw classifications; (a) Left step geometry, (b) right step geometry.

length is represented in the multiple of half flaw length "a". Figure 2 shows how ligament lengths and ligament angles are measured in multiple flaws specimens. The stress fields in the ligament area of right and left stepping geometries are different. The dominant stress field in the ligaments area of left or right stepping is tension or compression, respectively.[9]

3. Experimental Procedure and Results

The experiments are performed in uniaxial compressional loading until the load reaches failure of specimens. The loading is applied in a stepwise process at a constant displacement rate of 0.04 mm/minute. The loading is increased up to 10 kN (about 3.3 MPa of the specimens). At this point, the load is paused and the surface of the specimen is scanned for the first time. Afterwards, the loading is resumed and increased by 3 kN (about 1 MPa). Loading is paused at every 3 kN interval or when cracking sounds are heard. The surface of the specimen is inspected for possible crack initiation, propagation and coalescence. Scanning of the surface of the specimen is done with a low power microscope; a camera is attached to the microscope and the images are recorded in a VCR for later inspection. The type of crack initiated from any of the tips, initiation stress and angle, crack pattern, coalescence type and coalescence stress are the main observations made during testing. Two identical specimens for each geometry are prepared and tested to check repeatability. If the results from two identical tests show significant differences, a third specimen is prepared and tested. A total of 24 different types of flaw geometry have been investigated.

3.1 Cracks Initiation and Propagation

In uniaxial loading, wing cracks are observed in brittle and quasi-brittle materials such as, glass, PMMA, rocks, plaster of Paris, gypsum, and mortar.[7,10-14] From multiple flaws tests, wing cracks are observed. Cracks observed in sixteen flaws of gypsum in uniaxial compression are shown in Figure 3. Initiation of wing crack depends on flaw inclination angle; at a low flaw angle wing crack initiate near the tip of flaws and at the high flaw angle, wing cracks initiate from the tip of flaws. This type wing crack initiation in uniaxial compression

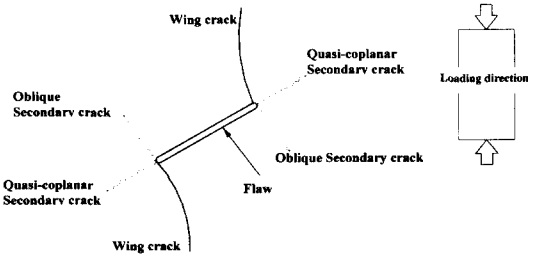

Fig. 3. Wing cracks and secondary cracks observed in sixteen flaw specimens.

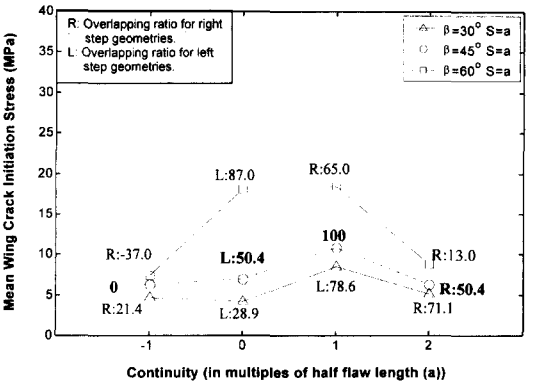

Fig. 4. Wing crack initiation stress with sixteen flaws, spacing = "a".

is also observed in PMMA by Barquins, and Petit.[11] In highly overlapping geometries, initiation of tensile crack is observed in the middle of flaws.

Propagation path of wing cracks follows maximum compressional direction and near the tip of flaw, propagation path is curvilinear as shown in Figure 3 because of mixed fracture mode condition. Along the path of wing crack, the fractography of wing crack shows very smooth and clean surface and no crushing is observed. Wing crack is easily detected because of its wide crack aperture and stable propagation.

Wing cracks are observed from all the tips of sixteen flaws and initiation of these cracks in a given flaw geometry is simultaneous. Figures 4, and 5 show effects of flaw geometries on wing crack initiation. They represent average wing crack initiation of spacing "a", and "2a". As they are shown, the initiation stress of wing crack increases with flaw inclination angle, overlapping ratio and spacing. Overlapping ratio is included in Figures 4 and 5, together with the types

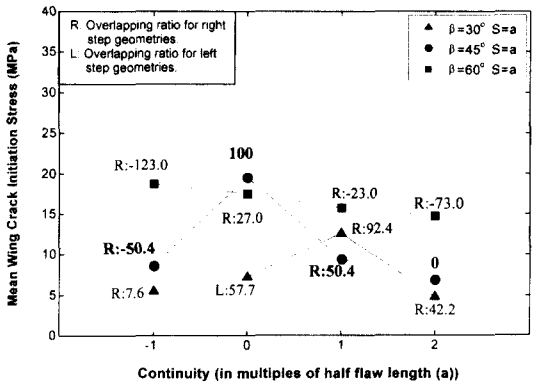

Fig. 5. Wing crack initiation stress with sixteen flaws, spacing = "2a".

of stepping: R for right stepping and L for left stepping. In the same condition of stepping and flaw inclination angle, increment of overlapping ratio shows higher initiation stress of wing cracks. This is analogous to the results from three flaws.[7]

Observation of secondary crack is more difficult than wing cracks. The aperture of secondary crack is less than micrometer so mostly they are observed with surface movement, i.e. spalling, or unstable movement before coalescence. The possible error induced by this may be severer than that of wing cracks. Two different types of secondary cracks, quasi-coplanar and oblique shear cracks, are observed from sixteen flaw tests like in two and three flaw tests (see Figure 3). Initiation of secondary cracks is stable near the onset but before coalescence, they propagate in an unstable manner. Initiation of quasi-coplanar secondary cracks is near coplanar to flaws and they are observed mainly in left stepping flaw geometry. Observation of oblique shear crack is first made in three flaw tests[7] and it appears in right stepping geometries only. Oblique secondary cracks propagate opposite direction to wing cracks (see Figure 3) and cause extra types of coalescence. Initiation stress of secondary cracks shows similar geometry dependency like wing cracks: increment of flaw inclination angle, spacing and overlapping ratio produce higher secondary crack initiation. Initiation stresses of wing and secondary cracks in sixteen flaws are lower than three flaws. It is expected results because increased number of flaws decreases strength of material and may produce different boundary condition.

3.2 Coalescence

Wing cracks and secondary cracks are the components of coalescence. Nine different types of coalescence from three flaws are summarized in Table 1. Two types of coalescence are added from past observation with seven types of coalescence.[7] Coalescence Type I is produced by the final unstable in-plane propagation and linkage of two quasi-coplanar secondary cracks. Coalescence Type II is produced by out of plane propagations of quasi-coplanar secondary cracks from the flaws, and the linkage with the unstable propagation of a tensile crack along the loading direction in the ligament area. Coalescence Type III occurs by the unstable propagation of the quasi-coplanar secondary crack from one of the flaws and linkage with the wing crack from the other flaw. Coalescence Type IV is a stable process that occurs through the propagation of the wing crack from one of the flaws. Coalescence Type V occurs through the unstable, out of plane propagation of one of the quasi-coplanar secondary cracks until it links with the quasi-coplanar secondary crack from the other flaw. The quasi-coplanar secondary crack propagates out of plane as a shear crack. These five types of coalescences are summarized in two flaw specimens.[6]

Coalescence Type VI is produced by the linkage of the wing crack from one of the flaws with the oblique secondary crack from the other flaw. Both wing and oblique secondary cracks propagate in a stable manner. Coalescence is produced by the stable propagation of the wing crack and linkage with the tip of the oblique secondary crack. This coalescence is quite similar to coalescence Type III since linkage is between a wing crack and a secondary crack. The difference is that in Type III linkage is through a quasi-coplanar crack in left stepping geometry, while in Type VI it is through an oblique secondary crack in right stepping geometry.

Coalescence Type VII occurs by the linkage of the oblique secondary crack from one of the flaws with the oblique secondary crack from the other flaw. The oblique secondary cracks initiate from the tips of the flaws and propagate in a stable manner. With further increase of loading, coalescence is produced in an abrupt manner with the linkage of the two oblique

Table 1. Types of coalescence in uniaxial compression in specimen with two and three flaws

Type	Left Stepping	Type	Right Stepping	Coalescence cracks
I	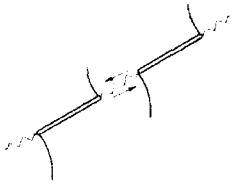	VI	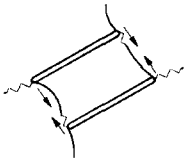	Type I: Quasi-coplanar secondary cracks. Type VI: Oblique secondary crack and wing crack.
II	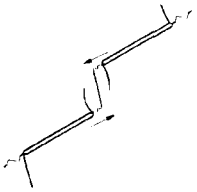	VII	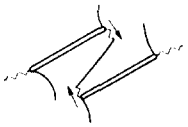	Type II: Quasi-coplanar secondary cracks and an out of plane tensile crack. Type VII: Oblique secondary cracks and an out of plane tensile crack.
III	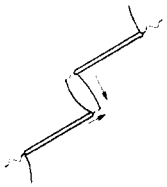	VIII		Type III: Quasi-coplanar secondary crack and wing crack. Type VIII: Oblique secondary cracks.
IV	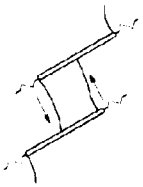	IX	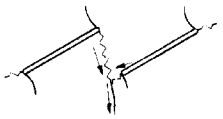	Type IV: Wing crack Type IX: Oblique secondary crack and quasi-coplanar secondary crack.
V	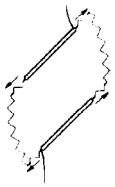			Type V: Quasi-coplanar secondary cracks and out of plane secondary shear crack.

secondary cracks by a tensile crack that runs diagonally with the plane of the flaws. Coalescence Type VII can be compared with Type II since in both cases the flaws are linked by an out of plane unstable propagation of a tensile crack. The difference between Type II and Type VII is that coalescence occurs by quasi-coplanar secondary cracks in left stepping geometries in Type II and by oblique secondary cracks in right stepping geometries in Type VII.

Coalescence Type VIII is caused by the linkage of two oblique secondary cracks. The oblique cracks initially propagate along their own plane in a stable manner. Coalescence is produced by the unstable propagation of one of the cracks. Coalescence Type VIII can be analogous to Type I. In both cases, linkage is produced by the unstable propagation of secondary cracks along their own plane. In Type VIII the secondary cracks are oblique while in Type I they are quasi-coplanar.

Coalescence Type IX is produced by the linkage of the quasi-coplanar secondary crack from one of the flaws with the oblique secondary crack from the other flaw. The initial propagation of both secondary cracks is stable up to near coalescence, where linkage occurs though the unstable propagation of the oblique secondary crack towards the quasi-coplanar crack. At

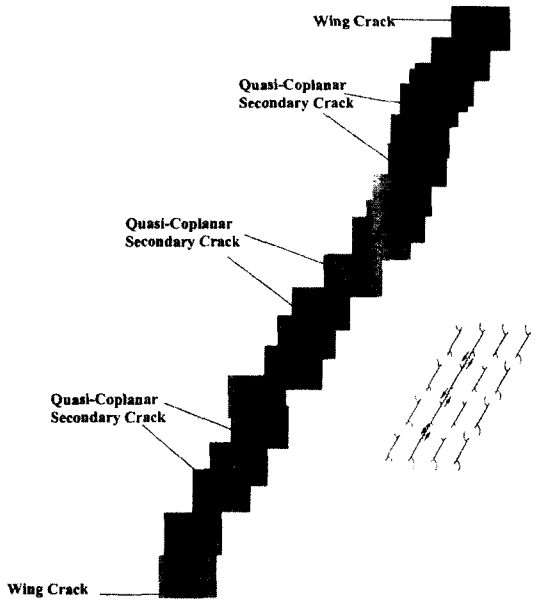

Fig. 6. Coalescence Type I. Specimen 2a-a60°.

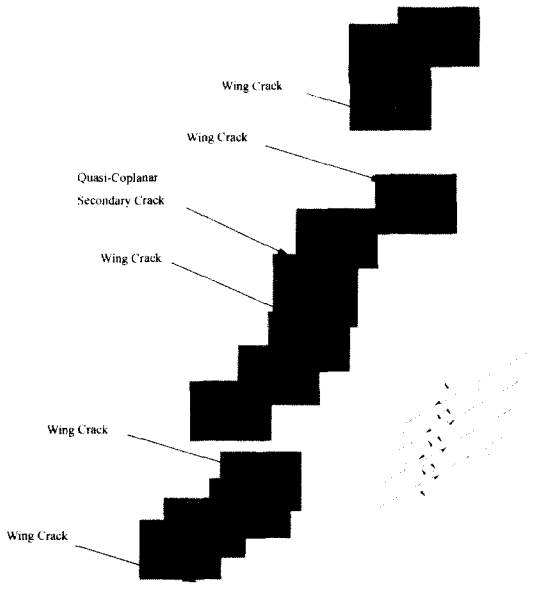

Fig. 7. Coalescence Type III. Specimen 2a030°.

the point of intersection of the two secondary cracks, a tensile crack is usually produced.

From nine different types of coalescence only four types of coalescence are observed in specimens with sixteen flaws, coalescence Types I, III, VI, and VII.

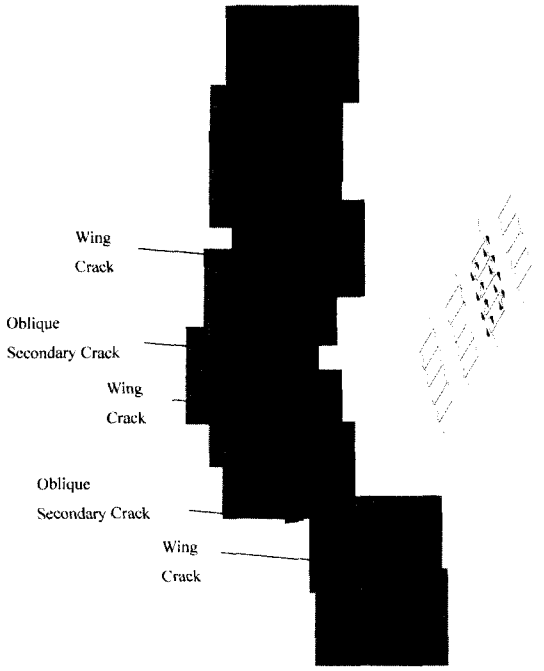

Fig. 8. Coalescence Type VI. Specimen aa60°.

The occurrence of coalescence in a specimen is in "columnar" direction except Type I coalescence. Coalescence Type I is observed in 2a-a60° (spacing-continuity-flaw inclination angle) flaw geometry and it is not repetitive like other types of coalescence (see Figure 6). Failure of the specimen is not right after the occurrence of coalescence Type I as shown in three flaws. The other rows of flaws, where no coalescence is found, can sustain additional load. Therefore, kinking steps on the coalescence can be more clearly seen because additional load applied dilate secondary crack surface. The complete of Type I coalescence is similar with what observed from three flaws geometry; stable initiation and propagation of quasi-coplanar secondary crack and unstable near the coalescence. Coalescence Type I is one of cross-columnar coalescence. Coalescence Type III is observed in flaw geometry of 2a030°, overlapping left stepping geometry (see Figure 7). Initiated wing crack links with a quasi-coplanar shear crack near the onset of the secondary crack. Coalescence Type VI is observed in aa60° flaw geometry (see Figure 8). This type of coalescence is observed in high overlapping ratio and right stepping

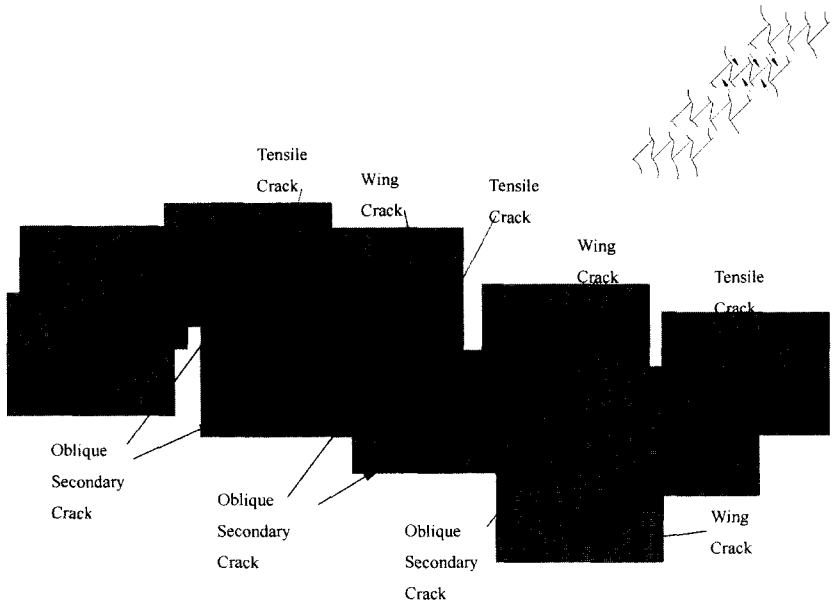

Fig. 9. Coalescence Types of VII. Specimen a-a45°.

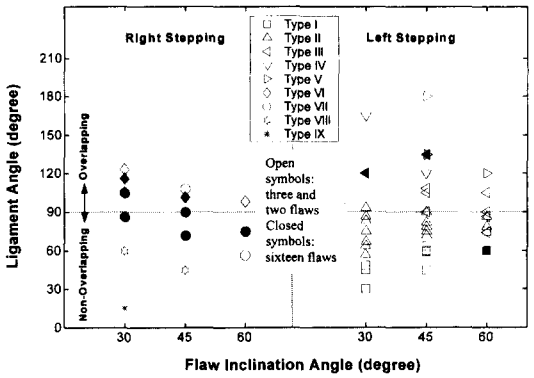

Fig. 10. Types of coalescence and flaw geometry for specimens with two, three and sixteen flaws.

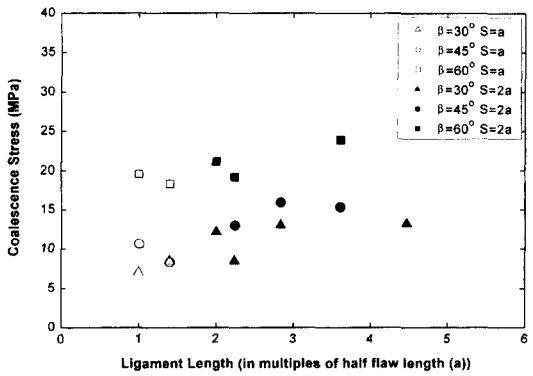

Fig. 11. Coalescence stress versus ligament length for specimens with sixteen flaws.

geometry. Wing crack propagates towards the onset of oblique secondary crack and produces coalescence Type VI. Propagation of oblique secondary cracks is steady and stable. Coalescence Type VII is observed in a-a45°, geometry with right stepping and relative low overlapping ratio (see Figure 9). Initiated oblique secondary cracks linked by out of plane tensile crack in the middle of ligament area. The occurrence of tensile crack is unstable.

The observed type of coalescence in sixteen flaws specimens correlates very well with the geometry of the flaws: flaw inclination angle, ligament angle, steppings. Figure 10 shows observed types of coalescence with respect to the ligament angle, flaw inclination angle and steppings in two, thee and sixteen flaws. Open symbols are the data from two and three flaws test results[6,7] and closed symbols are from sixteen flaws. Some of the data from two and three flaws in right stepping domain are blocked by closed symbols from sixteen flaws. Coalescence types can be grouped into each zone by different flaw geometry. Left stepping geometries favor coalescence Types I to V and

right stepping, Types VI to IX. Comparison between three and sixteen flaws shows that the types of coalescence observed in specimens with two and three flaws are the same as in specimens with sixteen flaws, if the flaw geometry is the same.

Figure 11 is a plot of the coalescence stress versus ligament length. The figure shows that, in general, coalescence stress increases with flaw inclination angle and with ligament length, up to a ligament length of about three times the half of a flaw length "3a". For larger ligament lengths, although there are few data, the coalescence stress appears to be rather constant. This may indicate that for smaller ligament lengths the interaction between the flaws is quite substantial, but beyond a certain distance such interaction is not significant. This observation is consistent with the results from experiments with two and three flaws.[6,7]

4. Conclusion

Extensive work on the fracture of multiple flaws, sixteen flaws, has been conducted on specimens made of gypsum under uniaxial compression. Generally, test results indicate that the fracturing process of sixteen flaws is akin to two and three flaws specimens. The followings are the most important conclusion from the observations:

Two different types of cracks are observed; wing and secondary cracks. Initiation of both crack is stable. Wing cracks and secondary cracks propagate in a stable manner. Secondary cracks show unstable propagation near coalescence. Different types of secondary cracks are observed: quasi-coplanar and oblique secondary cracks. Initiation and propagation direction of theses cracks are different: quasi-coplanar to the flaw (quasi-coplanar secondary cracks), and at an angle with the flaw (oblique secondary cracks). Wing crack and secondary crack initiation stress depend on the geometry of the flaws. The initiation stress increases with the flaw angle, with the spacing, and with the overlapping ratio. Increase of number of flaws decreases the strength of materials.

Four different types of coalescences are observed, Types I, III, VI, VII. The types of coalescence can be correlated with the geometry of the flaws: flaw inclination angle, ligament angle, and stepping. Coalescence in specimens with sixteen flaws tends to occur in a "columnar" pattern in which flaws in the same column are linked together. The coalescence stress increases with the flaw inclination angle and with the ligament length. For ligament lengths greater than "3a", the coalescence stress is quite constant and rather independent.

Limited number of geometries have been studied. Further works are required to understand the behavior of quasi-brittle rock material with discontinuities profoundly.

References

1. Goodman, R. E. and Kieffer, D. S., 2000, Behavior of rock in slopes, Journal of geotechnical engineering, 126 (8), 675-684.
2. Einstein, H. H., Veneziano, D., Baecher, G. B. and OReilly, K. J., 1993, The effect of discontinuity persistence on rock slope stability, International Journal of Rock Mechanics, Min. Sci., 20 (5), 227-236.
3. Du, W. and J. M. Kemeny., 1993, Modeling Borehole Breakout by Mixed Mode Crack Growth, Interaction and Coalescence, International Journal of Rock Mechanics, Min. Sci., 30 (7), 809-812.
4. Reyes, O. and Einstein, H. H., 1991, Failure mechanisms of fractured rock A fracture coalescence model, Proceedings 7th International Congress of Rock Mechanics, 1, 333-340.
5. Shen, B., Stephansson, O., Einstein, H. H. and Ghahreman, B., 1995, Coalescence, of fracture under shear stresses in experiments. Journal of Geophysical Research, 100 (B4) 5,975-5.990.
6. Bobet, A. and Einstein, H. H., 1998, Fracture coalescence in rock-type materials under uniaxial and biaxial compression, International Journal of Rock Mechanics, Min. Sci., 35 (7), 863-888.
7. Sagong, M. and Bobet, A., 2000, Coalescence of Multiple Flaws in Uniaxial Compression, Proceedings of the North American Rock Mechanics Symposium: Pacific Rocks 2000, 1,203-1,210.
8. Einstein, H. H. & Hirschfeld, R.C., 1970, Model studies on mechanics of jointed-rocks, ASCE Journal of the Geotechnical Division, 99, SM3, 229-248.
9. Vallejo, L.E., 1989, Fissure parameters in stiff clays under compression, ASCE Journal of Geotechnical Engineering, Vol. 115, No. 9, pp, 1,303-1,317.
10. Hoek, S. & Bieniawski, Z.T., 1984, Brittle fracture propagation in rock under compression. International Journal of Fracture, 26, 276-294.
11. Barquins, M. and J. P. Petit., 1992, Kinetic instabilities during the propagation of a branch crack: effects of

loading conditions and internal pressure, Journal of Structural Geology, 14(8/9), 893-903.
12. Ingraffea, A. R., 1985, Fracture Propagation in Rock, Mechanics of Geomaterials, 219-258.
13. Tasdemire, M. A., Maji, A. K., Shah, S. P., 1990, Crack Propagation in Concrete under Compression, Journal of Engineering Mechanics, 116(5), 1,058-1,076
14. Lajtai, E.Z., 1971, A theoretical and experimental evaluation of the Griffith theory of brittle fracture, Tectonophysics, 11, 129-156.

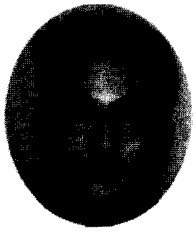

사공 명

1994년 한양대학교 토목공학과 공학학사
1998년 Purdue University 공학석사

Tel : 1-765-494-6242
E-mail : sagong@ecn.purdue.edu

현재 퍼듀대학교 토목공학과 박사 과정

안토니오 보베

현재 퍼듀대학교 토목 공학과 교수